Available online at http://scik.org
Commun. Math. Biol. Neurosci. 2022, 2022:59
https://doi.org/10.28919/cmbn/7375
ISSN: 2052-2541

HOST AND VECTOR MIGRATION ON THE SPREAD OF ANIMAL AFRICAN TRYPANOSOMIASIS: THE EFFECT OF SEASONAL VARIATION

MLYASHIMBI HELIKUMI[1,*], JACOB ISMAIL IRUNDE[2]

[1]Mbeya University of Science and Technology, Department of Mathematics and Statistics, College of Science and Technical Education, P.O. Box 131, Mbeya, Tanzania

[2]Department of Mathematics, Physics and Informatics, Mkwawa University College of Education, P.O. Box 2513 Iringa-Tanzania

Abstract. In this paper, a two patch-model for animal African trypanosomiasis (AAT) disease transmission that incorporates seasonal variation, livestock, wild animals and tsetse flies is proposed and studied. The main assumption in the formulated model is that seasonal variation is associated with migration of both hosts and vectors from one patch to another. From model analysis, we computed the basic reproduction number in a periodic environment. We noted that the disease can be eliminated in the population whenever the basic reproduction number is less than unity and exist whenever greater than one. We performed the numerical simulation of the model considering two scenarios: symmetrical and asymmetrical movement of hosts and vectors. Overall, we noted that migration of hosts and vectors have influence on the spread of disease in the population. Additionally, we observed that solution profile of all infected species is associated with periodic oscillations caused by the seasonal variations.

Keywords: African trypanosomiasis; mathematical model; seasonal variations; disease persistence; host migrations.

2010 AMS Subject Classification: 92C60.

*Corresponding author

E-mail address: mhelikumi@yahoo.co.uk

Received March 21, 2022

1. INTRODUCTION

Animal African Trypanosomiasis (AAT) is a devastating infection that is caused by protozoa of the Trypanosmoma genus. It is primarily transmitted by tsetse flies of the Glossina spp. to almost all domestic mammals and various wild mammal species [51]. The species of Trypanosmoma that can cause AAT include T. brucei congolense, T. brucei vivax, and T. brucei rhodesiense [52]. Although both animals and humans can be infected by T. brucei, the most affected are cattle because of the feeding preferences of tsetse flies [53].

Trypanosomiasis is one of the most important livestock diseases with devastating economic losses in Africa. In Sub-Saharan Africa (SSA), the direct and indirect impacts of the disease are estimated to approach 5 billion US dollars annually [54, 55]. The high mortality rates of livestock from this disease can cause up to a 50% annual reduction of milk and meat production in SSA [56]. According to Devèze [57], the AAT disease has pushed about half a million farmers in remote Africa to poverty. Apart from domestic cattle, the disease can also affect domestic swine, camels, goats, and sheep [58]. The infection of susceptible animals causes chronic or acute symptoms which are characterized by recurrent fever, diarrhea, anemia, and even death.

Substantial efforts have been made to study and control AAT but the disease persists in many parts of SSA [59]. Like other endemic diseases in SSA, mathematical models are among the efforts which have been explored to understand the dynamics of AAT in the region. Otieno et al. [60] assessed AAT dynamics in a cattle population and included wild animals as substitute tsetse fly feeding sources. The model showed that the disease was accelerated in the cattle population by the wild animals. Further analysis also demonstrated that the rates of vector biting and survival are significant parameters in the disease control strategies that aim to reduce contact between vector and cattle populations. Another model was developed by Kajunguri et al. [61] to include insecticide-treated cattle and the use of insecticides in the control of tsetse flies in a multi-host population. The authors established that the use of insecticides on cattle alongside the treatment of infected cattle and humans effectively decreased the prevalence of trypanosomes. Meisner et al. [62] modeled trypanocide treatment of cattle and demonstrated that as the number of trypanocide-treated cattle increased, the disease prevalence decreased.

Very recently, Lord et al. [63] assessed the effects of insecticide-treated cattle on the abundance of tsetse flies and trypanosome transmission at the livestock-wildlife interface in Serengeti, Tanzania, and estimated close to 30% increased tsetse fly mortality which explained the comparatively low prevalence of T. brucei in cattle. Ndondo et al. [14] also developed an AAT model but considered only treatment as a control strategy while excluding the contribution of host and vector migration and seasonal variations on the transmission of the disease.

Although numerous studies have been conducted to model the dynamics and control AAT, the infection still persists and affects animal production, and continues to threaten livelihoods and economic development in Africa. Most of the AAT models have not included seasonality as a factor that influences the transmission dynamics. Seasonal variations can change the rates of vector development, thus can influence the disease transmission dynamics [23]. The present paper aimed to incorporate the aspects of seasonal variations of vector and host migration in modelling the transmission of AAT to address the question "How do seasonal variations and migration of vector and host populations affect AAT transmission dynamics?" The paper is organized as follows: In Section 2, the model is formulated, and in Section 2.1, we compute the basic reproduction number and investigate the stability of the models' equilibria. In section 2.2, we perform the numerical simulations to verify the theoretical results and in Section 3, we have the concluding remarks concerning the formulated model.

2. MODEL FORMULATION

In this section, a two-patch model for the animal African trypanosomiasis (AAT) that incorporates seasonal variations, livestock, wild animals and tsetse flies is proposed and studied. Throughout the document we have used the subscripts L , W and V to denote the livestock, wild animals and vector respectively; the subscripts i and j represent the first and second patch for species with $i, j = 1,2$. The total population of livestock in patch i is denoted by $N_L i(t)$ with $i = 1,2$ which is sub-divided into four compartments: the susceptible $S_{Li}(t)$, exposed $E_{Li}(t)$, infected $I_{Li}(t)$ and recovered $R_{Li}(t)$ classes. Thus, the total population for livestock is given by $N_{Li}(t) = S_{Li}(t) + E_{Li}(t) + I_{Li}(t) + R_{Li}(t)$. The total population of wild animals in patch i is also sub-divided into susceptible $S_{Wi}(t)$, exposed $E_{Wi}(t)$, infected $I_{Wi}(t)$ and recovered $R_{Wi}(t)$ classes. Therefore, the total population of wild animals is given by

$N_{Wi}(t) = S_{Wi}(t) + E_{Wi}(t) + I_{Wi}(t) + R_{Wi}(t)$. Further more; the population of vectors in patch i is sub-divided into three compartments: susceptible $S_{Vi}(t)$, exposed $E_{Vi}(t)$ and infected $I_{Vi}(t)$. Thus, the total population of vectors is given by $N_{Vi}(t) = S_{Vi}(t) + E_{Vi}(t) + I_{Vi}(t)$. Both the livestock and wild animals acquire the AAT infection through contact with infected tsetse flies. On the other-hand, susceptible tsetse flies acquire infection through bites of an infected hosts (either livestock or wild animals). Therefore, the force of infection for livestock, wild animals and vectors in patch i are respectively denoted by λ_{Li}, λ_{Wi} and λ_{Vi} defined as:

$$\lambda_{Li}(t) = \frac{\sigma_{vi}(1-u_i)\beta_{VLi}I_{Vi}}{N_{Li}+N_{Wi}} \tag{1}$$

$$\lambda_{Wi}(t) = \frac{\sigma_{Vi}\beta_{VWi}I_{Vi}}{N_{Li}+N_{Wi}} \tag{2}$$

$$\lambda_{Vi}(t) = \frac{\sigma_{vi}(1-u_i)\beta_{LVi}I_{Li}}{N_{Li}+N_{Wi}} + \frac{\sigma_{Vi}\beta_{WVi}I_{Wi}}{N_{Li}+N_{Wi}} \tag{3}$$

The parameter β_{Vk} with $k = L, W$ represents the probability of disease transmission from infectious tsetse fly to susceptible hosts (either livestock or wild animal), $\sigma_{Vi}(t)$ represents a periodic function that accounts for vector biting rates and u_i represents the rate of spraying the livestock with insecticides to prevent contact with tsetse flies in patch i. Since most of the studies in literature (see,[5, 36]) show that seasonal variations influence the tsetse flies biting rates, we define the vector bite rates σ_{Vi} in patch i by:

$$\sigma_{Vi}(t) = \sigma^0_{Vi}[1 + \sigma^1_{Vi}\cos(\theta t + \tau)] \tag{4}$$

Where σ^0_{Vi} represents the average vector biting rate in the absence of seasonality, σ^1_{Vi} is a maximum amplitude of seasonal variations with $0 < \sigma^1_{Vi} < 1$, $\theta = \frac{2\pi}{360}$ define a one-year period and τ denotes the phase shift to capture the seasonality.

Following successive contact rates between hosts and vectors in patch i, the host becomes exposed and spend $\frac{1}{\alpha_{ki}}$ days in the incubation period. We have also assumed that infectious ki hosts in patch i recover from the infection with permanent immunity through treatment or naturally after $\frac{1}{\gamma_{ki}}$ days of infection. In addition, the parameters b_{ki} and μ_{ki} represent the birth and natural mortality rates of k hosts in patch i; β_{VL_i} and β_{VW_i} denote the probability of disease transmission from an infectious vector to susceptible livestock and wild animals in patch i; The change of

seasonality affects the life span of adult tsetse flies, and therefore, vectors may die while still in the incubation period. Therefore, we have assumed that upon infection, vectors progress to an infectious state at rate:

$$\alpha_{Vi}(t) = \alpha^0_{Vi}[1 + \alpha^1_{Vi}\cos(\theta t + \tau)] \tag{5}$$

where α^0_{Vi} denotes the average incubation rate in the absence of seasonal variations, α^1_{Vi} represents the maximum amplitude of seasonality with $0 < \alpha^0_{Vi} < 1$. In addition, $b_{Vi}(t)$ and $\mu_{Vi}(t)$ represent the vector birth and natural mortality rates respectively which both follow the seasonal variations:

$$b_{Vi}(t) = b^0_{Vi}[1 + b^1_{Vi}\cos(\theta t + \tau)] \tag{6}$$

$$\mu_{Vi}(t) = \mu^0_{Vi}[1 + \mu^1_{Vi}\cos(\theta t + \tau)] \tag{7}$$

Where μ^0_{Vi} and b^0_{Vi} denote the average natural mortality and birth rates, respectively, and $\mu^0_{Vi}(0 < \mu^0_{Vi} < 1)$ and $b^0_{Vi}(0 < b^0_{Vi} < 1)$ represent the maximum amplitudes of seasonal variations. In vector-borne diseases the abundance and distribution of both hosts and vectors, therefore, we have assumed that seasonality is associated with the migration of hosts and vectors from one patch to another. Let the migration of susceptible, exposed, and recovered livestock from patch i to j be denoted by $p_{ij}(t)$, while the migration of infectious livestock from patch i to j by $m_{ij}(t)$:

$$p_{ij}(t) = p^0_{ij}[1 + p^1_{ij}\cos(\theta t + \tau)] \tag{8}$$

$$m_{ij}(t) = m^0_{ij}[1 + m^1_{ij}\cos(\theta t + \tau)] \tag{9}$$

Where p^0_{ij}, m^1_{ij} denote the average movement rates in the absence of seasonal variations, $p^1_{ij}(0 < p^1_{ij} < 1)$ and $m^1_{ij}(0 < m^1_{ij} < 1)$ are the amplitudes of seasonal variations. The migration rate of susceptible, exposed and recovered wild animals in patch i to j is denoted by $q_{ij}(t)$, and that of infectious wild animals by $h_{ij}(t)$ which both follow the seasonal variations shown in (10) and (11):

$$q_{ij}(t) = q^0_{ij}[1 + q^1_{ij}\cos(\theta t + \tau)] \tag{10}$$

$$h_{ij}(t) = h^0_{ij}[1 + h^1_{ij}\cos(\theta t + \tau)] \tag{11}$$

Where q_{ij}^0, h_{ij}^1 denotes the average movement rates of wild animals in the absence of seasonal variations, $q_{ij}^1(0 < q_{ij}^1 < 1)$ and $h_{ij}^1(0 < h_{ij}^1 < 1)$ represent the maximum amplitudes of seasonality. Furthermore, $n_{ij}(t)$ is migration rate of susceptible and exposed vectors and $r_{ij}(t)$ the migration rate of infectious vectors. Therefore we define the movement rates for susceptible, exposed and infectious vectors from patch i to j by:

$$n_{ij}(t) = n_{ij}^0[1 + n_{ij}^1 \cos(\theta t + \tau)]$$

$$r_{ij}(t) = r_{ij}^0[1 + r_{ij}^1 \cos(\theta t + \tau)]$$

where n_{ij}^0, r_{ij}^1 represents the average migration rates in the absence of seasonal variations while $n_{ij}^1(0 < n_{ij}^1 < 1)$ and $r_{ij}^1(0 < r_{ij}^1 < 1)$ represent the maximum amplitude of seasonality. Based on the above assumptions, we have the following flow chart and nonlinear ordinary differential equations (for $i \neq j = 1, 2$):

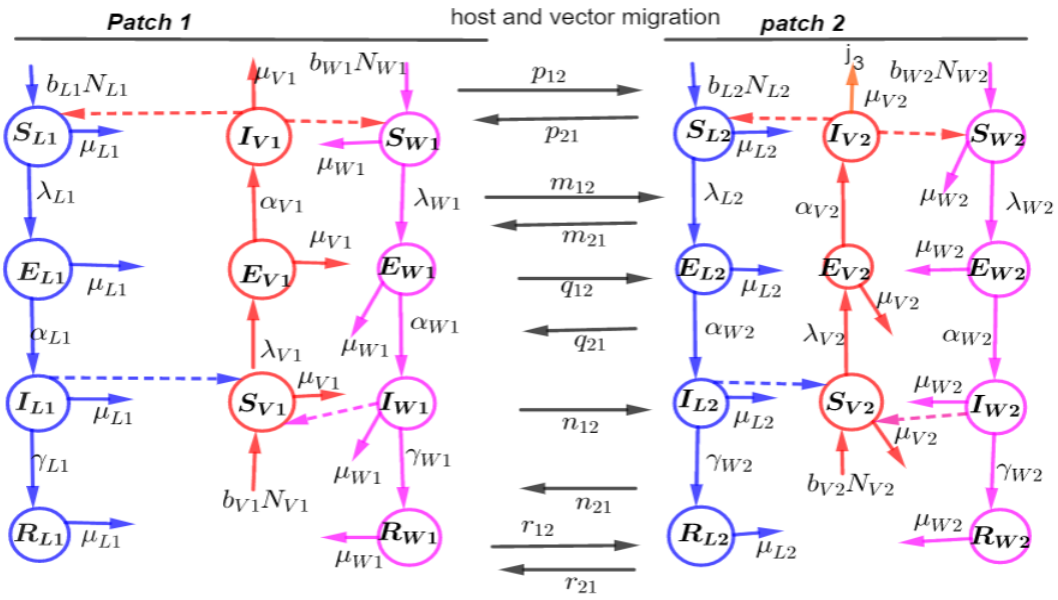

FIGURE 1. Flow chart of host and vector interactions

$$
(12)\quad \begin{cases}
S'_{Li}(t) &= b_{Li}N_{Li}(t) - \lambda_{Li}(t)S_{Li}(t) - \mu_{Li}S_{Li}(t) \\
&\quad + p_{ji}S_{Lj}(t) - p_{ij}S_{Hi}(t), \\
E'_{Li}(t) &= \lambda_{Li}(t)S_{Li}(t) - (\mu_{Li}+\alpha_{Li})E_{Li}(t) + p_{ji}E_{Lj}(t) - p_{ij}E_{Li}(t), \\
I'_{Li}(t) &= \alpha_{Li}E_{Li}(t) - (\mu_{Li}+\gamma_{Li})I_{Li}(t) + m_{ji}I_{Lj}(t) - m_{ij}I_{Li}(t), \\
R'_{Li}(t) &= \gamma_{Li}I_{Li}(t) - \mu_{Li}R_{Li}(t) + p_{ji}R_{Lj}(t) - p_{ij}R_{Li}(t), \\
S'_{Wi}(t) &= b_{Wi}N_{Wi}(t) - \lambda_{Wi}(t)S_{Wi}(t) - \mu_{Wi}S_{Wi}(t) \\
&\quad + q_{ji}(t)S_{qj}(t) - q_{ij}(t)S_{qi}(t), \\
E'_{Wi}(t) &= \lambda_{Wi}(t)S_{Wi}(t) - (\mu_{Wi}+\alpha_{Wi})E_{Wi}(t) + q_{ji}(t)E_{Wj}(t) - q_{ij}(t)E_{Wi}(t), \\
I'_{Wi}(t) &= \alpha_{Wi}E_{Wi}(t) - (\mu_{Wi}+\alpha_{Wi})I_{Wi}(t) + h_{ji}(t)I_{Wj}(t) - h_{ij}(t)I_{Wi}(t), \\
R'_{Wi}(t) &= \gamma_{Wi}I_{Wi}(t) - \mu_{Wi}R_{Wi}(t) + q_{ji}R_{Wj}(t) - q_{ij}R_{Wi}(t), \\
S'_{Vi}(t) &= b_{Vi}(t)N_{Vi}(t) - \lambda_{Vi}(t)S_{Vi}(t) - (\mu_{Vi}(t)+\delta_{Vi}(t))S_{Vi} \\
&\quad + n_{ji}(t)S_{Vj}(t) - n_{ij}(t)S_{Vi}(t), \\
E'_{Vi}(t) &= \lambda_{Vi}(t)S_{Vi}(t) - (\alpha_{Vi}(t)+\mu_{Vi}(t)+\delta_{Vi}(t))E_{Vi}(t) \\
&\quad + n_{ji}(t)E_{Vj}(t) - n_{ij}(t)E_{Vi}(t), \\
I'_{Vi}(t) &= \alpha_{Vi}(t)E_{Vi}(t) - (\mu_{Vi}(t)+\delta_{Vi}(t))I_{Vi}(t) + r_{ji}(t)I_{Vj}(t) - r_{ij}(t)I_{Vi}(t), \\
. &
\end{cases}
$$

2.1. The basic reproduction number. In this section, we compute the disease-free equilibrium followed by the threshold quantity R_0 which determines the power of the disease to invade the population. Therefore, by direct calculation, we have that the model system (12) is always has a disease-free equilibrium given by:

$$
\begin{aligned}
E^0 &= \left(S^0_{L1},0,0,0,S^0_{W1},0,0,0,S^0_{V1},0,0,S^0_{L2},0,0,0,S^0_{W2},0,0,0,S^0_{V2},0,0,\right) \\
&= (N_{L1},0,0,0,0,N_{W1},0,0,0,N_{V1},0,0,N_{L2},0,0,0,0,N_{W2},0,0,0,N_{V2},0,0)\,.
\end{aligned}
$$

Let $N_L(t)=\sum_{i=1}^{2}N_{Li}$, $N_W(t)=\sum_{i=1}^{2}N_{Wi}$, and $N_V(t)=\sum_{i=1}^{2}N_{Vi}$. Therefore, one can show that the domain of biological interest of the model system (12) given by:

$$
\Omega = \left\{ \begin{pmatrix} N_L(t) \\ N_W(t) \\ N_V(t) \end{pmatrix} \in \mathbb{R}^{22}_{+} \;\middle|\; \begin{array}{l} N_L(t) \le N_{L1}+N_{L2}, \\ N_W(t) \le N_{W1}+N_{W2}, \\ N_V(t) \le N_{V1}+N_{V2} \end{array} \right\},
$$

is positively invariant and attracts all orbits with respect to the model system (12), by the same approach as in Bacaër and Guernaoui [21] and the general calculation procedure in Wang and Zhao [22]. Therefore, we can similarly introduce the next-generation matrices $F(t)$ and $V(t)$ (evaluated at the disease-free equilibrium) as:

$$F(t) = \begin{bmatrix} F_1(t) & 0 \\ 0 & F_2(t) \end{bmatrix}, \quad \text{and} \quad V(t) = \begin{bmatrix} V_{11}(t) & V_{21}(t) \\ V_{12}(t) & V_{22}(t) \end{bmatrix} \tag{13}$$

where

$$F_i(t) = \begin{bmatrix} 0 & 0 & 0 & 0 & 0 & \dfrac{\sigma_{Vi}(t)(1-u_i)\beta_{VLi}N_{Li}}{N_{Li}+N_{Wi}} \\ 0 & 0 & 0 & 0 & 0 & 0 \\ 0 & 0 & 0 & 0 & 0 & \dfrac{\sigma_{Vi}(t)\beta_{VWi}N_{Wi}}{N_{Li}+N_{Wi}} \\ 0 & 0 & 0 & 0 & 0 & 0 \\ 0 & \dfrac{\sigma_{Vi}(t)(1-u_i)\beta_{LVi}N_{Vi}}{N_{Li}+N_{Wi}} & 0 & \dfrac{\sigma_{Vi}(t)\beta_{Wi}N_{Vi}}{N_{Li}+N_{Wi}} & 0 & 0 \\ 0 & 0 & 0 & 0 & 0 & 0 \end{bmatrix},$$

$$V_{11}(t) = \begin{bmatrix} y_1 & 0 & 0 & 0 & 0 & 0 \\ -\alpha_{L1} & y_2 & 0 & 0 & 0 & 0 \\ 0 & 0 & y_3 & 0 & 0 & 0 \\ 0 & 0 & -\alpha_{W1} & y_4 & 0 & 0 \\ 0 & 0 & 0 & 0 & y_5 & 0 \\ 0 & 0 & 0 & 0 & -\alpha_{V1}(t) & y_6 \end{bmatrix},$$

$$V_{22}(t) = \begin{bmatrix} x_1 & 0 & 0 & 0 & 0 & 0 \\ -\alpha_{L2} & x_2 & 0 & 0 & 0 & 0 \\ 0 & 0 & x_3 & 0 & 0 & 0 \\ 0 & 0 & -\alpha_{W2} & x_4 & 0 & 0 \\ 0 & 0 & 0 & 0 & x_5 & 0 \\ 0 & 0 & 0 & 0 & -\alpha_{V2}(t) & x_6 \end{bmatrix},$$

$$y_1 = \mu_{L1} + \alpha_{L1} + p_{12}(t), \qquad x_1 = \mu_{L2} + \alpha_{L2} + p_{21}(t),$$

$$
\begin{aligned}
y_2 &= \mu_{L1}+\gamma_{L1}+m_{12}(t), \qquad x_2=\mu_{L2}+\gamma_{L2}+m_{21}(t),\\
y_3 &= \mu_{W1}+\alpha_{W1}+q_{12}(t), \qquad x_3=\mu_{W2}+\alpha_{W2}+q_{21}(t),\\
y_4 &= \mu_{W1}+\gamma_{W1}+h_{12}(t), \qquad x_4=\mu_{W2}+\gamma_{W2}+h_{21}(t),\\
y_5 &= \mu_{V1}(t)+\alpha_{V1}(t)+\delta_{Vi}+n_{12}(t), \qquad x_5=\mu_{V2}(t)+\delta_{Vi}+\alpha_{V1}(t)+n_{21}(t),\\
y_6 &= \mu_{V1}(t)+\delta_{V1}+r_{12}(t), \qquad x_6=\mu_{V2}(t)+\delta_{V2}+r_{21}(t),
\end{aligned}
$$

and

$$
V_{12}(t)=\begin{bmatrix}
-p_{12} & 0 & 0 & 0 & 0 & 0\\
0 & -m_{12} & 0 & 0 & 0 & 0\\
0 & 0 & -q_{12}(t) & 0 & 0 & 0\\
0 & 0 & 0 & -h_{12}(t) & 0 & 0\\
0 & 0 & 0 & 0 & -n_{12}(t) & 0\\
0 & 0 & 0 & 0 & 0 & -r_{12}(t)
\end{bmatrix},
$$

$$
V_{21}(t)=\begin{bmatrix}
-p_{21} & 0 & 0 & 0 & 0 & 0\\
0 & -m_{21} & 0 & 0 & 0 & 0\\
0 & 0 & -q_{21}(t) & 0 & 0 & 0\\
0 & 0 & 0 & -h_{12}(t) & 0 & 0\\
0 & 0 & 0 & 0 & -n_{21}(t) & 0\\
0 & 0 & 0 & 0 & 0 & -r_{21}(t)
\end{bmatrix},
$$

In order to define the basic reproduction number of this non-autonomous model, we follow the work of Wang and Zhao [22] who introduced the next-infection operator L for a model in periodic environments by

$$
(L\phi)(t)=\int_0^{\infty} Z(t,t-s)F(t-s)\phi(t-s)ds, \tag{14}
$$

where $Z(t,s), t\geq s$, is the evolution operator of the linear ω-periodic system $dz/dt=-V(t)z$ and $\psi(t)$, while the initial distribution of infectious individuals is ω-periodic and nonnegative. The basic reproduction number is then defined as the spectral radius of the next-infection operator:

$$
R_0=\rho(L). \tag{15}
$$

For our model (12), the evolution operator can be determined by solving the system of differential equations $dz/dt = -V(t)z$ with the initial condition $Z(s,s) = I_{12\times 12}$. It can be easily verified that all entries of matrices $V_{12}(t)$ and $V_{21}(t)$ are zero. Further, we can simply $dz/dt = -V(t)z$ by considering $V_{11}(t)$ and $V_{22}(t)$ separately. Let $Z_{ii}(t,s)$ represent the outcome form $dz/dt = -V_{ii}(t)z$. Thus, we obtain:

$$Z_{11}(t,s) = \begin{bmatrix} y_{11}(t,s) & 0 & 0 & 0 & 0 & 0 \\ y_{21}(t,s) & y_{22}(t,s) & 0 & 0 & 0 & 0 \\ 0 & 0 & y_{33}(t,s) & 0 & 0 & 0 \\ 0 & 0 & y_{43}(t,s) & y_{44}(t,s) & 0 & 0 \\ 0 & 0 & 0 & 0 & y_{55}(t,s) & 0 \\ 0 & 0 & 0 & 0 & y_{65}(t,s) & y_{66}(t,s) \end{bmatrix}.$$

where:

$$\begin{aligned}
y_{11}(t,s) &= \exp-\left\{(\alpha_{L1}+\mu_{L1}+p_{12}^0)(t-s)+\frac{2p_{12}^0p_{12}^1}{\theta}\cos\left(\frac{\theta}{2}(t+s)\right)\sin\left(\frac{\theta}{2}(t-s)\right)\right\},\\
y_{21}(t,s) &= \left(e^{-\int(\mu_{L1}+\gamma_{L1}+m_{12}(t))dt}\right)\int_s^t e^{(\mu_{L1}+\alpha_{L1}+m_{12}(x))}\alpha_{L1}(x)y_{11}(x,s)dx,\\
y_{22}(t,s) &= \exp-\left\{(\gamma_{L1}+\mu_{L1}+m_{12}^0)(t-s)+\frac{2m_{12}^0m_{12}^1}{\theta}\cos\left(\frac{\theta}{2}(t+s)\right)\sin\left(\frac{\theta}{2}(t-s)\right)\right\},\\
y_{33}(t,s) &= \exp-\left\{(\alpha_{W1}+\mu_{W1}+q_{12}^0)(t-s)+\frac{2q_{12}^0q_{12}^1}{\theta}\cos\left(\frac{\theta}{2}(t+s)\right)\sin\left(\frac{\theta}{2}(t-s)\right)\right\},\\
y_{43}(t,s) &= \left(e^{-\int(\mu_{W1}+\gamma_{W1}+h_{12}(t))dt}\right)\int_s^t e^{(\mu_{W1}+\gamma_{W1}+h_{12}(x))}\gamma_{W1}(x)y_{33}(x,s)dx,\\
y_{44}(t,s) &= \exp-\left\{(\gamma_{W1}+\mu_{W1}+h_{12}^0)(t-s)+\frac{2h_{12}^0h_{12}^1}{\theta}\cos\left(\frac{\theta}{2}(t+s)\right)\sin\left(\frac{\theta}{2}(t-s)\right)\right\},\\
y_{55}(t,s) &= \exp-\left\{(\mu_{V1}^0+\alpha_{V1}^0+n_{12}^0+\delta_{V1})(t-s)+\frac{2\mu_{V1}^0\mu_{V1}^1}{\theta}\cos\left(\frac{\theta}{2}(t+s)\right)\sin\left(\frac{\theta}{2}(t-s)\right)\right.\\
&\quad +\frac{2\alpha_{V1}^0\alpha_{V1}}{\theta}\cos\left(\frac{\theta}{2}(t+s)\right)\sin\left(\frac{\theta}{2}(t-s)\right)\\
&\quad \left.+\frac{2n_{12}^0n_{12}^1}{\theta}\cos\left(\frac{\theta}{2}(t+s)\right)\sin\left(\frac{\theta}{2}(t-s)\right)\right\},\\
y_{65}(t,s) &= \left(e^{-\int(\mu_{V1}(t)+n_{12}(t)+\delta_{V1})dt}\right)\int_s^t e^{(\mu_{V1}(x)+n_{12}(x)+\delta_{V1})}\alpha_{V1}(x)y_{55}(x,s)dx,
\end{aligned}$$

$$
\begin{aligned}
y_{66}(t,s) &= \exp-\left\{\mu_{V1}^0(t-s)+\frac{2\mu_{V1}^0\mu_{V1}^1}{\theta}\cos\left(\frac{\theta}{2}(t+s)\right)\sin\left(\frac{\theta}{2}(t-s)\right)\right.\\
&\left.+r_{12}^0(t-s)+\frac{2r_{12}^0r_{12}^1}{\theta}\cos\left(\frac{\theta}{2}(t+s)\right)\sin\left(\frac{\theta}{2}(t-s)\right)+\delta_{V1}(t-s)\right\},
\end{aligned}
$$

.

and:

$$
Z_{22}(t,s)=\begin{bmatrix}
x_{11}(t,s) & 0 & 0 & 0 & 0 & 0\\
x_{21}(t,s) & x_{22}(t,s) & 0 & 0 & 0 & 0\\
0 & 0 & x_{33}(t,s) & 0 & 0 & 0\\
0 & 0 & x_{43}(t,s) & x_{44}(t,s) & 0 & 0\\
0 & 0 & 0 & 0 & x_{55}(t,s) & 0\\
0 & 0 & 0 & 0 & x_{65}(t,s) & x_{66}(t,s)
\end{bmatrix}.
$$

where:

$$
\begin{aligned}
x_{11}(t,s) &= \exp-\left\{(\alpha_{L2}+\mu_{L2}+p_{21}^0)(t-s)+\frac{2p_{21}^0p_{21}^1}{\theta}\cos\left(\frac{\theta}{2}(t+s)\right)\sin\left(\frac{\theta}{2}(t-s)\right)\right\},\\
x_{21}(t,s) &= \left(e^{-\int(\mu_{L2}+\gamma_{L2}+m_{21}(t))dt}\right)\int_s^t e^{(\mu_{L2}+\alpha_{L2}+m_{21}(x))}\alpha_{L2}(x)x_{11}(x,s)dx,\\
x_{22}(t,s) &= \exp-\left\{(\gamma_{L2}+\mu_{L2}+m_{21}^0)(t-s)+\frac{2m_{21}^0m_{21}^1}{\theta}\cos\left(\frac{\theta}{2}(t+s)\right)\sin\left(\frac{\theta}{2}(t-s)\right)\right\},\\
x_{33}(t,s) &= \exp-\left\{(\alpha_{W2}+\mu_{W2}+q_{21}^0)(t-s)+\frac{2q_{21}^0q_{21}^1}{\theta}\cos\left(\frac{\theta}{2}(t+s)\right)\sin\left(\frac{\theta}{2}(t-s)\right)\right\},\\
x_{43}(t,s) &= \left(e^{-\int(\mu_{W2}+\gamma_{W2}+h_{21}(t))dt}\right)\int_s^t e^{(\mu_{W2}+\gamma_{W2}+h_{21}(x))}\gamma_{W2}(x)x_{33}(x,s)dx,\\
x_{44}(t,s) &= \exp-\left\{(\gamma_{W2}+\mu_{W2}+h_{21}^0)(t-s)+\frac{2h_{21}^0h_{21}^1}{\theta}\cos\left(\frac{\theta}{2}(t+s)\right)\sin\left(\frac{\theta}{2}(t-s)\right)\right\},\\
x_{55}(t,s) &= \exp-\left\{(\mu_{V2}^0+\alpha_{V2}^0+n_{21}^0+\delta_{V2})(t-s)+\frac{2\mu_{V2}^0\mu_{V2}^1}{\theta}\cos\left(\frac{\theta}{2}(t+s)\right)\sin\left(\frac{\theta}{2}(t-s)\right)\right.\\
&+\frac{2\alpha_{V2}^0\alpha_{V2}}{\theta}\cos\left(\frac{\theta}{2}(t+s)\right)\sin\left(\frac{\theta}{2}(t-s)\right)\\
&\left.+\frac{2n_{21}^0n_{21}^1}{\theta}\cos\left(\frac{\theta}{2}(t+s)\right)\sin\left(\frac{\theta}{2}(t-s)\right)\right\},
\end{aligned}
$$

$$
\begin{aligned}
x_{65}(t,s) &= \left(e^{-\int(\mu_{V2}(t)+n_{21}(t)+\delta_{V2})dt}\right)\int_s^t e^{(\mu_{V2}(x)+n_{21}(x)+\delta_{V2})}\alpha_{V2}(x)x_{55}(x,s)dx,\\
x_{66}(t,s) &= \exp-\left\{\mu^0_{V2}(t-s)+\frac{2\mu^0_{V2}\mu^1_{V2}}{\theta}\cos\left(\frac{\theta}{2}(t+s)\right)\sin\left(\frac{\theta}{2}(t-s)\right)\right.\\
&\quad \left.+r^0_{21}(t-s)+\frac{2r^0_{12}r^1_{21}}{\theta}\cos\left(\frac{\theta}{2}(t+s)\right)\sin\left(\frac{\theta}{2}(t-s)\right)+\delta_{V2}(t-s)\right\},
\end{aligned}
$$

.

In what follows, we use the same approach as in Helikumi at el. [23] to analyze the threshold parameter defined in Equation (15). We use lemma 1 to demonstrate that the threshold parameter R_{0i} is the local stability for the disease-free equilibrium E^0.

Lemma 1. *(Theorem 2.2 in Wang and Zhao* [22]*). Suppose that $Z(t) = (E_{ji}(t), I_{ji}(t))$, with $i = 1,2$ and $j = L,W,V$ denote the species of all infected classes for the model system (12), such that its linearization at disease-free equilibrium E^0 is:*

$$\dot{Z}(t) = (F_i(t) - V_{ii}(t))z(t), \tag{16}$$

where $F_i(t)$ and $V_{ii}(t)$ represent the matrix for singular (14). Furthermore, let $\phi_{F_i(t)-V_{ii}(t)}$ and $\rho(\phi_{F_i-V_{ii}(\xi)}$ be the monodromy matrix of system (16) and the spectral radius of $\phi_{F_i-V_{ii}}(\xi)$, respectively. Then we have following statements:

(i) $R_{0i} = 1$, *if and only if* $\rho(\phi_{F_i-V_{ii}}(\xi)) = 1$;

(ii) $R_{0i} > 1$, *if and only if* $\rho(\phi_{F_i-V_{ii}}(\xi)) > 1$;

(iii) $R_{0i} < 1$, *if and only if* $\rho(\phi_{F_i-V_{ii}}(\xi)) < 1$.

Therefore, the disease-free equilibrium E^0 of the model system (12) is locally asymptotically stable if $R_{0i} < 1$ and unstable if $R_{0i} > 1$.

In what follows, we have to show that the threshold quantity R_{0i} which determines the ability of AAT to invade the population is an important threshold parameter for disease extinction and persistence. In particular, we have to demonstrate that when $R_{0i} < 1$, the model system (12) admits a globally asymptotically stable disease-free equilibrium E^0, and if $R_{0i} > 1$, the disease

persists and we use the same approach as in [46]. First of all we stare and prove the theorem (2.1):

Theorem 2.1. *If $R_{0i} < 1$ with $i = 1,2$, then the disease-free equilibrium E^0 of system (12) is globally asymptotically stable in Ω.*

Proof. According to Lemma 1, if $R_{0i} < 1$, then the disease-free equilibrium E^0 of the model system (12) is locally asymptotically stable. Therefore, we demonstrate that for $R_0 < 1$, the disease-free equilibrium is the global attractor. Assume that $R_0 < 1$, again from Lemma 1, we have, $\rho(\xi_{F-V}(\phi)) < 1$. By considering the infected classes, we have the following outcome for $i \neq j = 1,2$:

$$\begin{cases}
\dot{E}_{Hi}(t) & \leq & \left(\dfrac{\sigma_{Vi}(t)(1-u_i)\beta_{VLi}I_{Vi}}{N_{Li}(t)+N_{Wi}(t)}\right)S^0_{Li} - (\mu_{Li}+\alpha_{Li})E_{Li}(t) + p_{ji}E_{Lj}(t) - p_{ij}E_{Li}(t), \\
\dot{I}_{Li}(t) & = & \alpha_{Li}E_{Li}(t) - (\mu_{Li}+\gamma_{Li})I_{Li}(t) + m_{ji}I_{Lj}(t) - m_{ij}I_{Li}(t), \\
\dot{E}_{Wi}(t) & \leq & \left(\dfrac{\sigma_{Vi}(t)\beta_{VWi}I_{Vi}}{N_{Li}(t)+N_{Wi}}\right)S^0_{Wi} - (\mu_{Wi}+\alpha_{Wi})E_{Wi}(t) + q_{ji}(t)E_{Wj}(t) - q_{ij}(t)E_{Wi}(t), \\
\dot{I}_{Wi}(t) & = & \alpha_{Wi}E_{Wi}(t) - (\mu_{Wi}+\alpha_{Wi})I_{Wi}(t) + h_{ji}(t)I_{Wj}(t) - h_{ij}(t)I_{Wi}(t), \\
\dot{E}_{Vi}(t) & \leq & \left(\dfrac{\sigma_{Vi}(t)(1-u_i)\beta_{LVi}I_{Li}}{N_{Li}(t)+N_{Wi}} + \dfrac{\sigma_{Vi}(t)\beta_{WVi}I_{Wi}}{N_{Li}(t)+N_{Wi}}\right)S^0_{Vi} + (\alpha_{Vi}(t)+\mu_{Vi}(t)+\delta_{Vi}(t))E_{Vi}(t) \\
& & +n_{ji}(t)E_{Vj}(t) - n_{ij}(t)E_{Vi}(t), \\
\dot{I}_{Vi}(t) & = & \alpha_{Vi}(t)E_{Vi}(t) - (\mu_{Vi}(t)+\delta_{Vi}(t))I_{Vi}(t) + r_{ji}(t)I_{Vj}(t) - r_{ij}(t)I_{Vi}(t).
\end{cases}$$

for $t \geq 0$. Consider the following auxiliary system:

$$\begin{cases}
\dot{\widetilde{E}}_{Li}(t) & = & \left(\dfrac{\sigma_{Vi}(t)(1-u_i)\beta_{VLi}\widetilde{I}_{Vi}}{N_{Li}(t)+N_{Wi}(t)}\right)S^0_{Li} - (\mu_{Li}+\alpha_{Li})\widetilde{E}_{Li}(t) + p_{ji}\widetilde{E}_{Lj}(t) - p_{ij}\widetilde{E}_{Li}(t), \\
\dot{\widetilde{I}}_{Li}(t) & = & \alpha_{Li}\widetilde{E}_{Li}(t) - (\mu_{Li}+\gamma_{Li})\widetilde{I}_{Li}(t) + m_{ji}\widetilde{I}_{Lj}(t) - m_{ij}\widetilde{I}_{Li}(t), \\
\dot{\widetilde{E}}_{Wi}(t) & = & \left(\dfrac{\sigma_{Vi}(t)\beta_{VWi}\widetilde{I}_{Vi}}{N_{Li}(t)+N_{Wi}}\right)S^0_{Wi} - (\mu_{Wi}+\alpha_{Wi})\widetilde{E}_{Wi}(t) + q_{ji}(t)\widetilde{E}_{Wj}(t) - q_{ij}(t)E_{Wi}(t), \\
\dot{\widetilde{I}}_{Wi}(t) & = & \alpha_{Wi}\widetilde{E}_{Wi}(t) - (\mu_{Wi}+\alpha_{Wi})\widetilde{I}_{Wi}(t) + h_{ji}(t)\widetilde{I}_{Wj}(t) - h_{ij}(t)\widetilde{I}_{Wi}(t), \\
\dot{\widetilde{E}}_{Vi}(t) & = & \left(\dfrac{\sigma_{Vi}(t)(1-u_i)\beta_{LVi}\widetilde{I}_{Li}}{N_{Li}(t)+N_{Wi}} + \dfrac{\sigma_{Vi}(t)\beta_{WVi}\widetilde{I}_{Wi}}{N_{Li}(t)+N_{Wi}}\right)S^0_{Vi} + (\alpha_{Vi}(t)+\mu_{Vi}(t)+\delta_{Vi}(t))\widetilde{E}_{Vi}(t) \\
& & +n_{ji}(t)\widetilde{E}_{Vj}(t) - n_{ij}(t)\widetilde{E}_{Vi}(t), \\
\dot{\widetilde{I}}_{Vi}(t) & = & \alpha_{Vi}(t)\widetilde{E}_{Vi}(t) - (\mu_{Vi}(t)+\delta_{Vi}(t))\widetilde{I}_{Vi}(t) + r_{ji}(t)\widetilde{I}_{Vj}(t) - r_{ij}(t)\widetilde{I}_{Vi}(t).
\end{cases}$$

By Lemma 1 and the standard comparison principle, there exists a positive $\omega-$periodic function $\widetilde{z}(t)$ such that $z(t) \leq \widetilde{z}(t)e^{pt}$, where $\widetilde{z}(t) = (\widetilde{E}_{ij}(t), \widetilde{I}_{ij}(t), \widetilde{R}_{kj})^{\mathrm{T}}$, for $i = L,W,V$, $j = 1,2$, $k = L,W$, and $p = \frac{1}{\xi} \ln \rho\left(\phi_{(F-V)(\cdot)}(\xi)\right) < 0$. Thus, we conclude that $y(t) \to 0$ as $t \to \infty$, that is:

$$\lim_{t\to\infty} E_{ij}(t) = 0, \quad \lim_{t\to\infty} I_{ij}(t) = 0, \quad \text{and} \qquad \lim_{t\to\infty} R_{kj}(t) = 0, \qquad i = L,,W, j = 1,2, k = L,W.$$

Hence it follows that:

$$\lim_{t\to\infty} S_{ij}(t) = S^0_{ij}, \qquad \text{and} \qquad \lim_{t\to\infty} N_{ij}(t) = N^0_{ij}, \qquad i = L,W,V, \quad j = 1,2.$$

Thus, we conclude that the disease-free equilibrium E^0 of system (12) is globally asymptotically stable. □

Theorem 2.2. *If $R_0 > 1$, then system (12) is uniformly persistent, i.e., there exists a positive constant η, such that for all initial values of $(S_{ij}(0), E_{ij}(0), I_{ij}(0), R_k(0))\mathbb{R}^5_+ \times Int(\mathbb{R}_+)^6$, ($i = L,W,V$, $j = 1,2$, $k = L,W$), the solution of model (12) satisfies:*

$$\liminf_{t\to\infty} S_{ij}(t) \geq \eta, \quad \liminf_{t\to\infty} E_{ij}(t) \geq \eta, \quad \liminf_{t\to\infty} I_{ij}(t) \geq \eta, \quad \liminf_{t\to\infty} R_k(t) \geq \eta.$$

Proof. Let consider the following:

$$Z = \mathbb{R}^{12}_+; \qquad Z_0 = \mathbb{R}^6_+ \times \mathrm{Int}(\mathbb{R}_+)^6; \qquad \partial Z_0 = Y \backslash Z_0.$$

Let $P : Z \longrightarrow Z$ be the Poincaré map associated with our model (12), such that $P(z_0) = u(\omega, z_0)$ $\forall z_0 \in Z$, where $u(t, z_0)$ denotes the unique solution of the system with $u(0, z_0) = z_0$. Therefore, we fist show that P is uniformly persistent with respect to $(Z_0, \partial Z_0)$. From model (12), Z and Z_0 are positively invariant. Moreover, ∂Z_0 is a relatively closed set in Z. It follows from Theorem 2.2 that solutions of model (12) are uniformly and ultimately bounded. Thus the semiflow P is point dissipative on $\mathbb{R}^{11}_+$, and $P : \mathbb{R}^{11}_+ \to \mathbb{R}^{11}_+$ is compact. By Theorem 3.4.8 in [47] it then follows that P admits a global attractor which attracts every bounded set in $\mathbb{R}^{11}_+$.
Define:

$$N_\partial = \{(S_{ij}(0), E_{ij}(0), I_{ij}(0), R_k(0)) \in \partial Y_0 : \ P^n(S_{ij}(0), E_{ij}(0), I_{ij}(0), R_k(0)) \in \partial Y_0, \ \forall m \geq 0\},$$

for $i = L,W,V, \quad j = 1,2 \quad k = L,W.$

Next, we claim that $N_\partial = \{(S_{Lj}(0),0,0,R_{Lj}(0),S_{Wj}(0),0,0,R_{Wj}(0),S_{Vj}(0),0,0) : S_{ij} \geq 0, R_k \geq 0\}$. Clearly, $\widetilde{N} = \{(S_{Lj}(0),0,0,R_{Lj}(0),S_{Wj}(0),0,0,R_{Wj}(0),S_{Vj}(0),0,0) : S_{ij} \geq 0, R_k \geq 0\} \subseteq N_\partial$. Now, for any $(S_{ij}(0),\ E_{ij}(0),\ I_{ij}(0),R_k(0)) \in \partial Z_0 \backslash N$; if $E_{Lj}(0) = I_{Lj}(0) = 0$, it follows that $S_{ij}(0) > 0$, $R_{Lj}(0) > 0$, $E_{Wj}(0) > 0$, $I_{Wj}(0) > 0$, $R_{Wj}(0) > 0$, $E_{Vj}(0) > 0$, $I_{Vj}(0) > 0$, $\dot{E}_{Lj}(0) = \lambda_{Lj}(0)S_{Lj}(0) > 0$, and $\dot{I}_{Lj}(0) = 0$. If $E_{Wj}(0) = I_{Wj}(0) = 0$, it follows that $S_{ij}(0) > 0$, $E_{Lj}(0) > 0$, $I_{Lj}(0) > 0$, $R_{Lj}(0) > 0$, $R_{Wj}(0) = 0$, $E_{Vj}(0) > 0$, $I_{Vj}(0) > 0$, $\dot{E}_{Wj}(0) = \lambda_{Wj}(0)S_{Wj}(0) > 0$, and $\dot{I}_{Wj}(0) = 0$. If $E_{Vj}(0) = I_vVj(0) = 0$, it follows that $S_{ij}(0) > 0$, $E_{Lj}(0) = 0$, $I_{Lj}(0) = 0$, $R_{Lj}(0) > 0$, $E_{Wj}(0) = 0$, $I_{Wj}(0) = 0$, $R_{Wj}(0) = 0$, $\dot{E}_{Vj}(0) = 0$, and $\dot{I}_{Wj}(0) = 0$. Thus, we have $(S_{ij}(0),E_{ij}(0),I_{ij}(0),R_k(0)) \notin \partial Z_0$ for $0 < t \ll 1$. By the positive invariance of Z_0, we know that $P^n(S_{ij}(0),E_{ij}(0),I_{ij}(0),R_k(0)) \notin \partial Z_0$ for $n \geq 1$, hence $(S_{ij}(0),E_{ij}(0),I_{ij}(0),R_k(0)) \notin N_\partial$, and thus, $N_\partial = \{(S_{Lj}(0),0,0,R_{Lj}(0),S_{Wj}(0),0,0,R_{Wj}(0),S_{Vj}(0),0,0) : S_{ij} \geq 0, R_k \geq 0\}$.
Now consider the fixed point: $N_0 = (S^0_{Lj},0,0,R^0_{Lj},S^0_{Wj},0,0,0,S^0_{Vj},0,0)$ of the Poincaré map P, and define $W^S(N_0) = \{z_0 : P^n(z_0) \to N_0, n \to \infty\}$. We show that:

$$W^S(N_0) \cap z_0 = \emptyset. \tag{17}$$

Based on the continuity of solutions with respect to the initial conditions, for any $\varepsilon > 0$, there exists $\delta > 0$ small enough such that for all $(S_{ij}(0),E_{ij}(0),I_{ij}(0),R_k(0)) \in Z_0$ with $||(S_iij(0),E_{ij}(0),I_{ij}(0),R_k(0)) - N_0|| \leq \delta$, we have:

$$||f(t,(S_{ij}(0),E_{ij}(0),I_{ij}(0),R_k(0)) - f(t,N_0)|| < \varepsilon, \quad \forall t \in [0,\omega].$$

To obtain (17), we claim that:

$$\limsup_{m\to\infty} ||P^n(S_i(0),E_{ij}(0),I_{ij}(0),R_k(0)) - N_0|| \geq \delta, \quad \forall (S_{ij}(0),E_{ij}(0),I_{ij}(0),R_k(0)) \in Y_0.$$

We prove this claim by contradiction; that is, we suppose $\limsup_{m\to\infty} ||P^n(S_{ij}(0),E_{ij}(0),I_{ij}(0),R_k(0)) - N_0|| < \delta$ for some $(S_{ij}(0),E_{ij}(0),I_{ij}(0),R_k(0)) \in Y_0$. Without loss of generality, we assume that $||P^n(S_{ij}(0),E_{ij}(0),I_{ij}(0),R_k(0)) - N_0|| < \delta, \ \forall m \geq 0$. Thus,

$$||f(t,P^n(S_{ij}(0),E_{ij}(0),I_{ij}(0),R_k(0)) - f(t,N_0)|| < \varepsilon, \quad \forall t \in [0,\xi] \text{ and } n \geq 0.$$

Moreover, for any $t \geq 0$, we write $t = t_0 + q\xi$ with $t_0 \in [0, \xi$ and $q = [\frac{t}{\xi}]$, the greatest integer less than or equal to $\frac{t}{\xi}$. Then we obtain:

$$||f(t,(S_{ij}(0),E_{ij}(0),I_{ij}(0),R_k(0)) - f(t,N_0)|| = ||f(t_0,P^n(S_{ij}(0),E_{ij}(0),I_{ij}(0),R_k(0)) - f(t_0,N_0)|| < \varepsilon$$

for any $t \geq 0$. Let $(S_{ij}(t),E_{ij}(t),I_{ij}(t),R_k(t)) = f(t,(S_{ij}(0),E_{ij}(0),I_{ij}(0),R_k(0))$. It follows that $N_{ij}^0 - \varepsilon < S_{ij}(t) < N_{ij}^0 + \varepsilon$, $0 < E_{ij}(t) < \varepsilon$, $0 < I_{ij}(t) < \varepsilon$, and $0 < R_k(t) < \varepsilon$. By considering infected classes only, we have the following relations:

$$\begin{aligned}
\frac{dE_{Li}}{dt} &= \frac{\sigma_{Vi}(t)(1-u_i)\beta_{VLi}I_{Vi}S_{Li}}{N_{Li}+N_{Wi}} - (\mu_{Li}+\alpha_{Li})E_{Li}(t) + p_{ji}E_{Lj}(t) - p_{ij}E_{Li}(t),\\
&\geq \frac{\sigma_{Vi}(t)(1-u_i)\beta_{VLi}I_{Vi}(N_{Li}^0-\varepsilon)}{(N_{Li}^0+\varepsilon)+(N_{Wi}^0+\varepsilon)} - (\mu_{Li}+\alpha_{Li})E_{Li}(t) + p_{ji}E_{Lj}(t) - p_{ij}E_{Li}(t),\\
&= \left(\frac{\sigma_{Vi}(t)(1-u_i)\beta_{VLi}N_{Li}^0}{N_{Li}^0+N_{Wi}^0}\right)\left(\frac{1-\frac{\varepsilon}{N_{Li}^0+N_{Wi}^0}\left(1+\frac{N_{Wi}^0}{N_{Li}^0}\right)}{1+\frac{2\varepsilon}{N_{Li}^0+N_{Wi}^0}}\right)I_{Vi} - (\mu_{Li}+\alpha_{Li})E_{Li}(t) +\\
&\quad p_{ji}E_{Lj}(t) - p_{ij}E_{Li}(t).
\end{aligned}$$

For clinically infected humans we have:

$$\dot{I}_{Li}(t) = \alpha_{Li}E_{Li}(t) - (\mu_{Li}+\gamma_{Li})I_{Li}(t) + m_{ji}I_{Lj}(t) - m_{ij}I_{Li}(t).$$

The equations of the exposed animal populations become:

$$\begin{aligned}
\frac{dE_{Wi}}{dt} &= \frac{\sigma_{Vi}(t)\beta_{VWi}I_{Vi}S_{Wi}}{N_{Wi}+N_{Wi}} - (\mu_{Wi}+\alpha_{Wi})E_{Wi}(t) + q_{ji}E_{Wj}(t) - q_{ij}E_{Wi}(t),\\
&\geq \frac{\sigma_{Vi}(t)\beta_{VWi}I_{Vi}(N_{Wi}^0-\varepsilon)}{(N_{Wi}^0+\varepsilon)+(N_{Wi}^0+\varepsilon)} - (\mu_{Wi}+\alpha_{Wi})E_{Wi}(t) + q_{ji}E_{Wj}(t) - q_{ij}E_{Wi}(t),\\
&= \left(\frac{\sigma_{Vi}(t)\beta_{VWi}N_{Wi}^0}{N_{Wi}^0+N_{Wi}^0}\right)\left(\frac{1-\frac{\varepsilon}{N_{Li}^0+N_{Wi}^0}\left(1+\frac{N_{Wi}^0}{N_{Wi}^0}\right)}{1+\frac{2\varepsilon}{N_{Wi}^0+N_{Wi}^0}}\right)I_{Vi} - (\mu_{Wi}+\alpha_{Wi})E_{Wi}(t) +\\
&\quad q_{ji}E_{Wj}(t) - q_{ij}E_{Wi}(t).
\end{aligned}$$

For infectious animals, we have the following outcome:

$$\dot{I}_{Wi}(t) = \alpha_{Wi}E_{Wi}(t) - (\mu_{Wi}+\alpha_{Wi})I_{Wi}(t) + h_{ji}(t)I_{Wj}(t) - h_{ij}(t)I_{Wi}(t).$$

The equations for the exposed vectors are given by:

$$\begin{aligned}
\frac{dE_{Vi}}{dt} &\geq \frac{\sigma_{Vi}(t)(1-u_i)\beta_{LVi}I_{Li}(N^0_{Vi}-\varepsilon)}{(N^0_{Li}+\varepsilon)+(N^0_{Ai}+\varepsilon)} + \frac{\sigma_{Vi}(t)\beta_{WVi}I_{Wi}(N^0_{V1}-\varepsilon)}{(N^0_{Vi}+\varepsilon)+(N^0_{Wi}+\varepsilon)} \\
&\quad -(\alpha_{Vi}(t)+\mu_{Vi}(t)+\delta_{Vi})E_{Vi}(t) + n_{ji}(t)E_{Vj}(t) - n_{ij}(t)E_{Vi}(t), \\
&= \left(\frac{\sigma_{Vi}(t)(1-u_i)\beta_{VLi}N^0_{Li}}{N^0_{Li}+N^0_{Wi}}\right)\left(\frac{1-\frac{\varepsilon}{N^0_{Li}+N^0_{Wi}}\left(1+\frac{N^0_{Wi}}{N^0_{Li}}\right)}{1+\frac{2\varepsilon}{N^0_{Li}+N^0_{Wi}}}\right)I_{Vi} \\
&\quad + \left(\frac{\sigma_{Vi}(t)\beta_{VWi}N^0_{Wi}}{N^0_{Wi}+N^0_{Wi}}\right)\left(\frac{1-\frac{\varepsilon}{N^0_{Li}+N^0_{Wi}}\left(1+\frac{N^0_{Wi}}{N^0_{Wi}}\right)}{1+\frac{2\varepsilon}{N^0_{Wi}+N^0_{Wi}}}\right)I_{Vi} \\
&\quad -(\alpha_{Vi}(t)+\mu_{Vi}(t)+\delta_{Vi}(t))E_{Vi}(t) + n_{ji}(t)E_{Vj}(t) - n_{ij}(t)E_{Vi}(t).
\end{aligned}$$

Finally, the equations for infected vectors are given by:

$$\dot{I}_{Vi}(t) = \alpha_{Vi}(t)E_{Vi}(t) - (\mu_{Vi}(t)+\delta_{Vi}(t))I_{Vi}(t) + r_{ji}(t)I_{Vj}(t) - r_{ij}(t)I_{Vi}(t).$$

For $i = 1, 2$, let

$$M^i_\varepsilon = \begin{bmatrix}
0 & 0 & 0 & 0 & 0 & \left(\frac{\frac{\varepsilon}{N^0_{Li}+N^0_{Wi}}\left(1+\frac{N^0_{Wi}}{N^0_{Li}}\right)}{1+\frac{2\varepsilon}{N^0_{Li}+N^0_{Wi}}}\right) \\
0 & 0 & 0 & 0 & 0 & 0 \\
0 & 0 & 0 & 0 & 0 & \left(\frac{\frac{\varepsilon}{N^0_{Li}+N^0_{Wi}}\left(1+\frac{N^0_{Wi}}{N^0_{Wi}}\right)}{1+\frac{2\varepsilon}{N^0_{Wi}+N^0_{Wi}}}\right) \\
0 & 0 & 0 & 0 & 0 & 0 \\
0 & \left(\frac{\frac{\varepsilon}{N^0_{Li}+N^0_{Wi}}\left(1+\frac{N^0_{Wi}}{N^0_{Li}}\right)}{1+\frac{2\varepsilon}{N^0_{Li}+N^0_{Wi}}}\right) & 0 & \left(\frac{\frac{\varepsilon}{N^0_{Li}+N^0_{Wi}}\left(1+\frac{N^0_{Wi}}{N^0_{Wi}}\right)}{1+\frac{2\varepsilon}{N^0_{Wi}+N^0_{Wi}}}\right) & 0 & 0 \\
0 & 0 & 0 & 0 & 0 & 0
\end{bmatrix},$$

such that:

$$[\dot{E}_{Li}, \quad \dot{I}_{Li}, \quad \dot{E}_{Wi}, \quad \dot{I}_{Wi}, \quad \dot{E}_{Vi}, \quad \dot{I}_{Vi}]^{\mathrm{T}} \geq [F - V - M_{\varepsilon}^{i}][E_{Li}, \quad I_{Wi}, \quad E_{Wi}, \quad I_{Wi}, \quad E_{Vi}, \quad I_{Vi}]^{\mathrm{T}}.$$

Again based on [22, Theorem 2.2], we know that if $\rho(\Phi_{F-V}(\omega)) > 1$, then we can choose ε small enough such that $\rho(\Phi_{F-V-M_{\varepsilon}}(\omega)) > 1$. Again by [22, Theorem 2.2] and the standard comparison principle, there exists a positive $\omega-$ periodic function $v(t)$ such that $z(t) \geq \widetilde{z}_1(t)e^{p_1 t}$, where $\widetilde{z}_1(t) = (\widetilde{E}_{Lji}(t), \widetilde{I}_{Lji}(t))^{\mathrm{T}}$, for $j = W, L, V$, $i = 1, 2$ and $p_1 = \frac{1}{\xi}\ln\rho\left(\phi_{(F-V-M_{\varepsilon})}(\xi)\right) > 0$ which implies that:

$$\lim_{t\to\infty} E_i(t) = \infty, \qquad \text{and} \qquad \lim_{t\to\infty} I_j(t) = \infty, \quad j = L, W, V.$$

which is a contradiction in N_{∂} since N_{∂} converges to N_0 and N_0 is acyclic in N_{∂}. By [49, Theorem 1.3.1], for a stronger repelling property of ∂Z_0, we conclude that P is uniformly persistent with respect to $(Z_0, \partial Z_0)$, which implies the uniform persistence of the solutions of system (12) with respect to $(Z_0, \partial Z_0)$ [49, Theorem 3.1.1]. □

3. NUMERICAL RESULTS

The following assumed initial population levels for each patch will be considered: $S_{Li} = 10000$, $E_{Li} = 40$, $I_{Li} = 20$, $R_{Li} = 0$, $S_{Wi} = 10000$, $E_{Wi} = 40$, $I_{Wi} = 20$, $R_{Wi} = 0$, $S_{Vi} = 20000$, $E_{Vi} = 20$, $I_{Vi} = 10$. Furthermore, the rest of the parameter values used were taken from Table 1, a majority of which values were adopted from the works of Moore et al. [5] and Ndondo et al. [14], while a few were assumed within realistic ranges due to their unavailability. The total number of new infections generated per patch over a time period $t \in [0, t_f]$ for human and cattle populations were determined by the following formulas respectively:

$$\begin{cases} C_{Li} &= \displaystyle\int_0^{t_f} \left(\frac{\sigma_{Vi}(t)(1-u_i)\beta_{VLi} I_{Vi}(t)}{N_{Li}(t) + N_{Wi}(t)} \right) dt, \\ \\ C_{Wi} &= \displaystyle\int_0^{t_f} \left(\frac{\sigma_{Vi}(t)\beta_{VWi} I_{Vi}(t)}{N_{Li}(t) + N_{Wi}(t)} \right) dt, \end{cases}$$

and:

TABLE 1. Description of model parameters of system (12), indicating baseline, ranges and references.

Symbol	Description	Value	Unit	Source
N_{L1}, N_{L2}	Total livestock animal population size	1000	Livestock	[5]
N_{W1}, N_{W2}	Total wild animals size	2000	Animals	[5]
N_{V1}, N_{V2}	Total tsetse population size	6000	Tsetse flies	[5]
τ	Phase-shifting parameter	50	Days	Assumed
b_{Wi}, b_{Wi}	Birth rate for the hosts	$\frac{1}{15\times365}, \frac{1}{50\times365}$	Day^{-1}	[14]
b^0_{Vi}	Average birth rate of the vectors	$\frac{1}{33}$	Day^{-1}	[14]
μ^0_{Vi}	Average mortality rate of the vectors	$\frac{1}{33}$	Day^{-1}	[14]
μ_{Wi}, μ_{Li}	Natural mortality rate for the hosts	$\frac{1}{15\times365}, \frac{1}{50\times365}$	Day^{-1}	[14]
κ^0_{Vi}	Average incubation rate for the vectors	$\frac{1}{25}(\frac{1}{25}-\frac{1}{30})$	Day^{-1}	[14]
κ_{Wi}, κ_{Li}	Incubation rate for the hosts	$\frac{1}{12}(\frac{1}{10}-\frac{1}{14})$	Day^{-1}	[14]
σ^0_{Vi}	Average vector biting rate	$\frac{1}{4}(\frac{1}{10}-\frac{1}{3})$	Day^{-1}	[14]
α_{Wi}, α_{Li}	Recovery rate of the infectious host	$\frac{1}{25}, \frac{1}{30}$	Day^{-1}	[14]
η	Relative tsetse preference for animal hosts	25		[5]
γ_{Wi}, γ_{Li}	Immunity waning rate for the recovered host	$\frac{1}{75}, \frac{1}{90}$	Day^{-1}	[14]
β_{VWi}, β_{VLi}	Probability of infection from an infectious vector to a susceptible host given that a contact between the two occurs	0.62		[14]
β_{WVi}, β_{LVi}	Probability that a vector becomes infected after biting an infectious animal or human	0.01		[14]
p_{ij}	Migration rate of un-infected livestock from patch j to i	varied	Day^{-1}	
m_{ij}	Migration rate of infected livestock from patch j to i	varied	Day^{-1}	
q^0_{ij}	Migration rate of un-infected wild animals from patch j to i	varied	Day^{-1}	
h^0_{ij}	Migration rate of infected wild animals from patch j to i	varied	Day^{-1}	
n^0_{ij}	Average migration rate of vectors from patch j to i	varied	Day^{-1}	

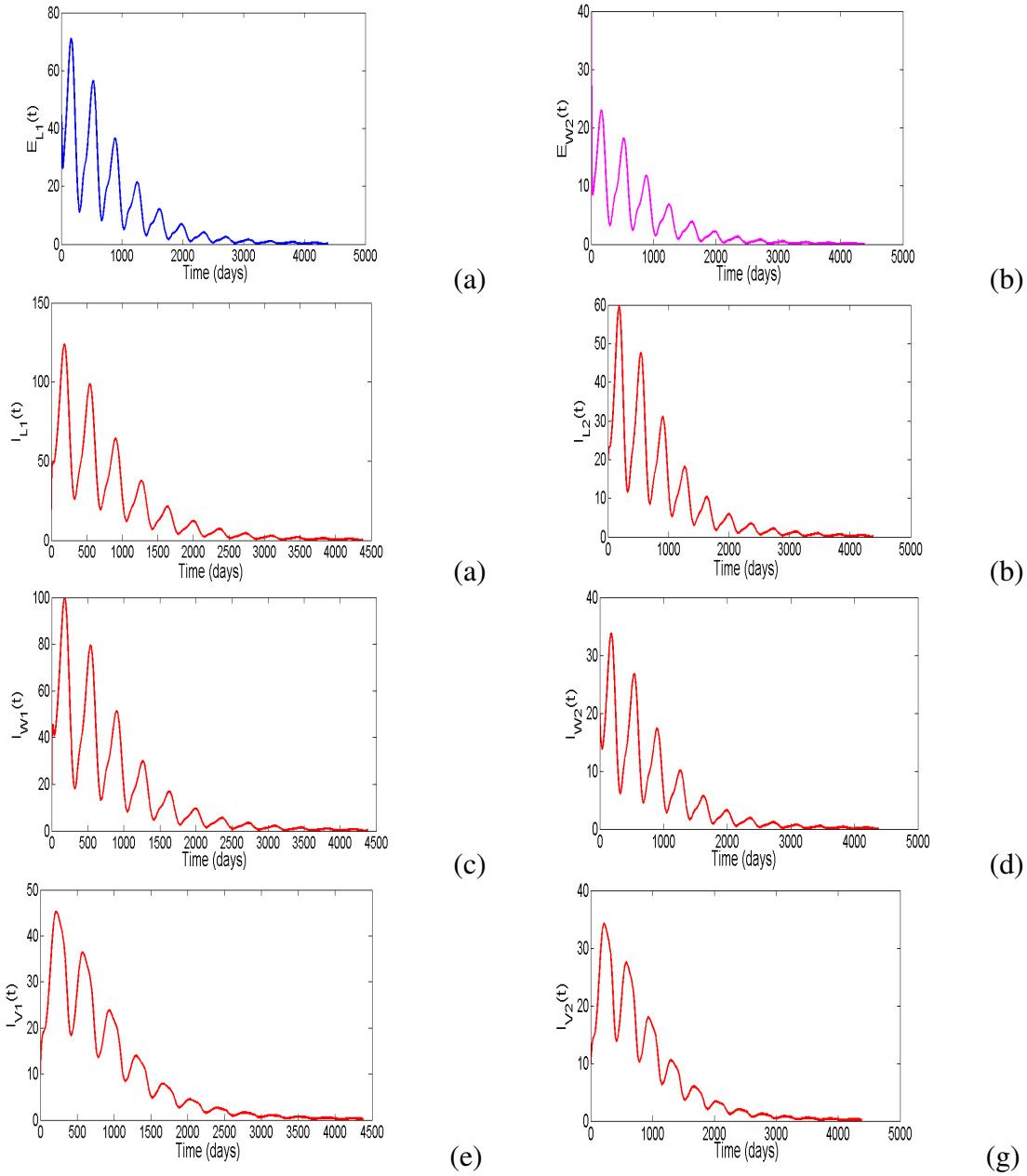

FIGURE 2. Numerical simulations showing the effect of seasonality on the dynamics of AAT disease.

3.0.1. *Scenario 1-asymmetrical movement of the livestock, wild animals and tsetse flies.*

In Fig. 2, we simulated the model system (12) to show the effects of seasonality with asymmetrical migration for both hosts and vectors. We assumed that the migration rate of livestock, wild animals, and vectors in patch 2 is higher than in patch 1. We used the value of parameters in Table 1 to simulate the model and migration rates in patch 1 and 2 was set to be $m_{12} = 0.1$, $m_{21} = 0.2$, $n_{12} = 0.1$, $n_{21} = 0.13$, $p_{12} = 0.1$, $p_{21} = 0.3$, $q_{12} = 0.1$, $q_{21} = 0.3$, $h_{12} = 0.1$, $h_{21} = 0.13$. From the numerical simulations, we observed that the number of new infections for the livestock in patch 1 and 2 are 3.7993×10^3 and 958.5724 respectively. Additionally, we observed that the solution profile of all infected species is associated with periodic oscillations caused by change of seasonality.

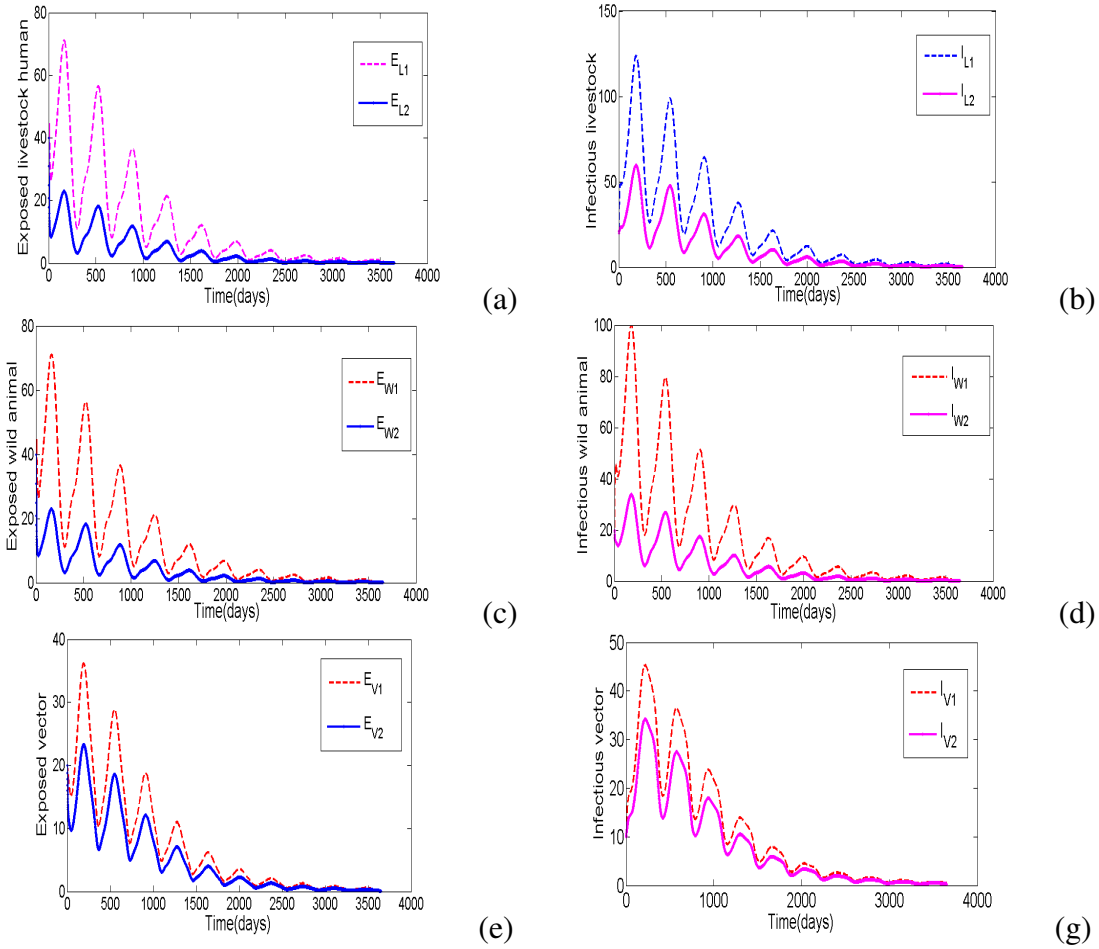

FIGURE 3. Numerical simulations showing the effect of host and vector migrations

In Fig. 3, we performed the numerical simulations for the model system (12) to demonstrate the effects of migration of livestock, wild animals and vectors on the spread of African trypanosomiasis disease transmission. We have assumed that the rate of movement of livestock, wild animals, and vectors in patch 2 is higher than in patch 1. We used the value of parameters in Table 1 to simulate the model and set $m_{12} = 0.1$,$m_{21} = 0.2$, $n_{12} = 0.1$, $n_{21} = 0.13$, $p_{12} = 0.1$, $p_{21} = 0.3$, $q_{12} = 0.1$, $q_{21} = 0.3$, $h_{12} = 0.1$, $h_{21} = 0.13$. Overall, we noted that new infections for the livestock population in patches 1 and 2 are 3.7758×10^3 and 952.6599 respectively. On the other hand, the total number of new infections for wild animal in both patches is 3.7513×10^3. The results has an implication that migration rate of livestock, wild animals and vectors from one patch to another influence the spread of disease in the populations.

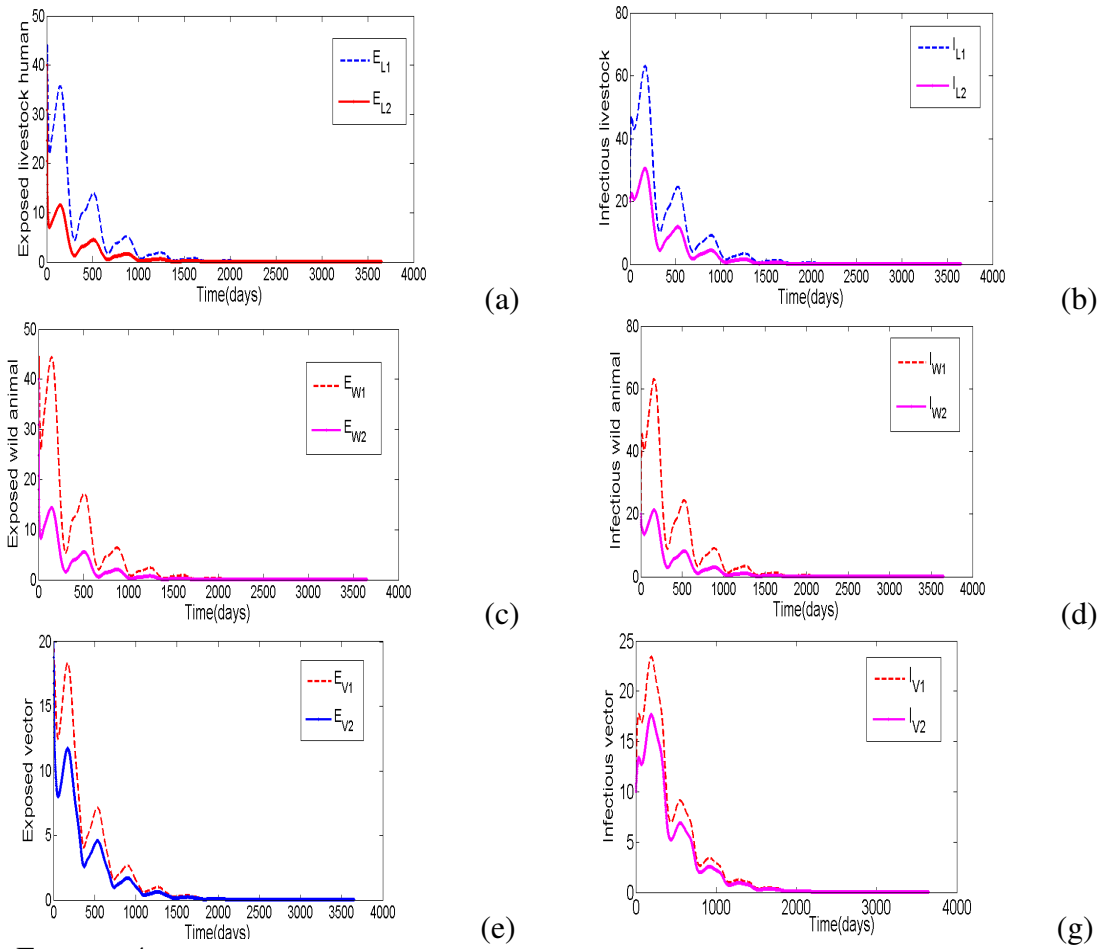

FIGURE 4. Numerical simulation showing the effects of treating livestock with $u_1 = u_2 = 0.2$

In Fig. 4, we simulated the model system (12) to show the effect of insecticides on spread of animal trypanosomiasis. We assumed the same rate of treating the livestock in both patches, that is $u_1 = u_2 = 0.2$ and compared the results with those in Fig. 3. Overall, one can note that the number of new infections generated in patches 1 and 2 is 1.0432×10^3 and 264 respectively, which is low compared to the number of infections in Fig. 3. Additionally, the number of new infections generated for wild animals in both patches is 1.2926×10^3, which is less compared to the number of infections in Fig. 3. This demonstrate that treating the livestock with insecticides in both patches have the potential to reduce the spread of disease in the populations.

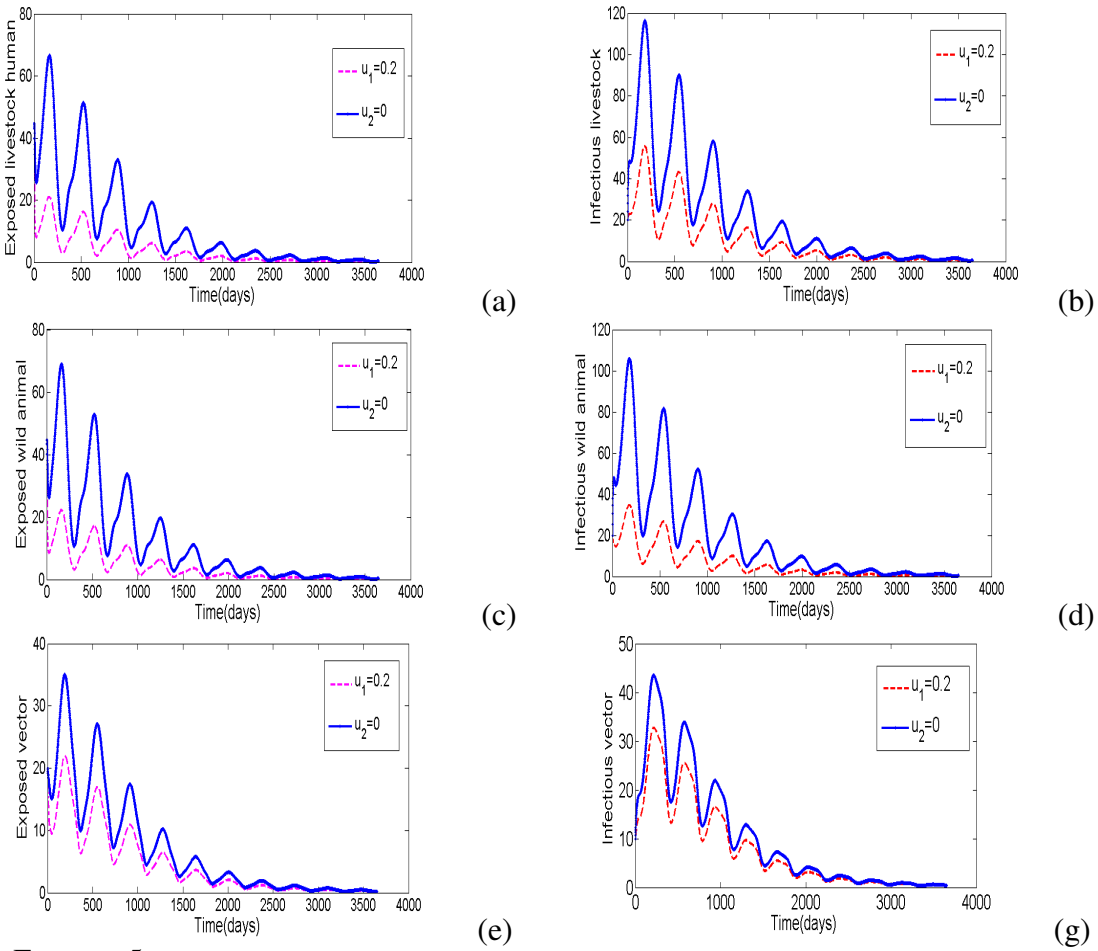

FIGURE 5. Numerical simulation showing the effect of treating the livestock with insecticide spray, with $u_1 = 0.2$ in patch 1 and $u_2 = 0$ in patch 2

3.0.2. *Scenario 2-symmetrical movement of the livestock, wild animals and tsetse flies.*

In Fig. 5, we simulated the model system (12) to show the impact of treating livestock with insecticides spray. We assumed the same rates of animal migration in both patches. We assigned the control in patch 1 to be $u_1 = 0.2$ and that of patch 2 to be $u_1 = 0$. we observed that, the number of new infections generated in patch 1 was low compared to patch 2. In particular, we observed that the number of new infections in patch 1 was 723 and that of patch 2 was 3.5946×10^3. On the other hand, the number of new infection for wild animals in both patches was 895. From the results one can note that treating the livestock with insecticide spray reduce the spread of disease in the populations.

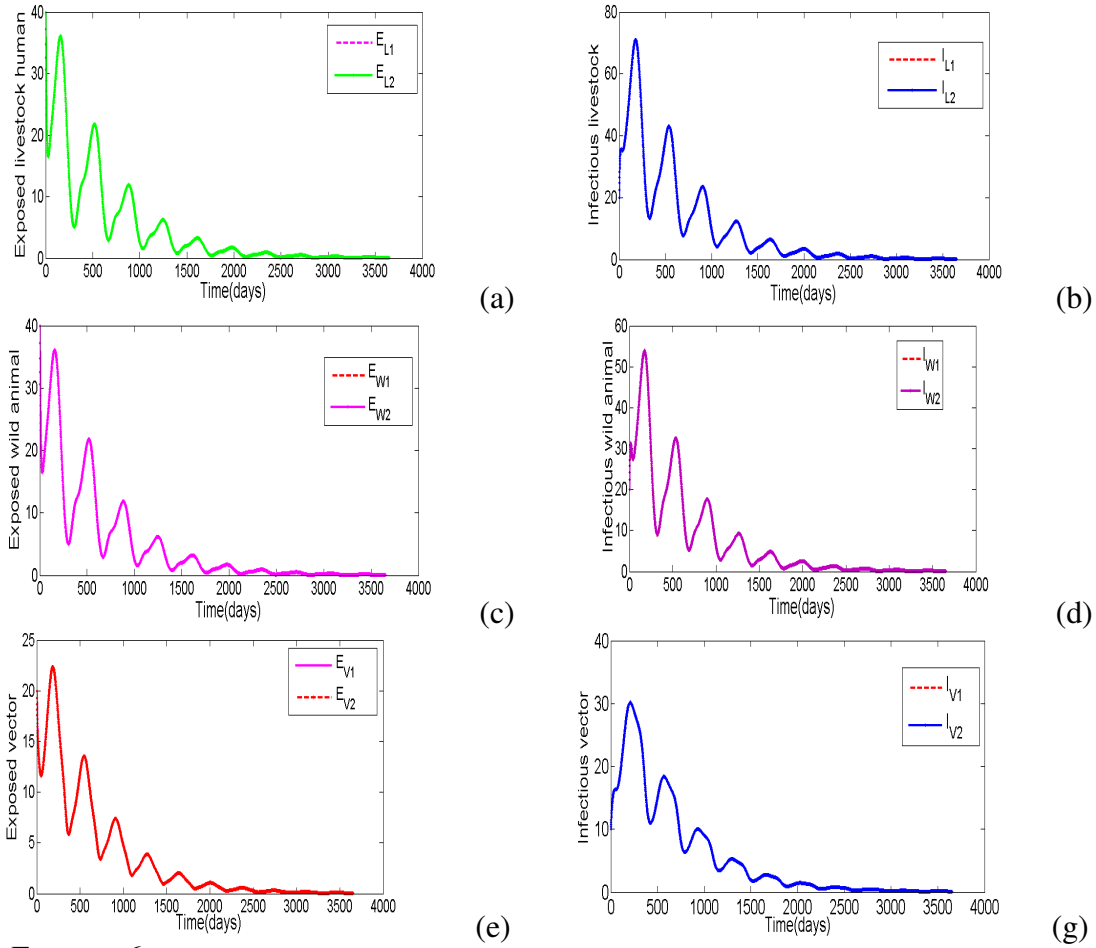

FIGURE 6. Numerical simulations showing the effects of host and vector migrations with $u_1 = u_2 = 0$.

In Fig. 6, shows the effect of symmetric movement for both hosts and vectors in the dynamics of animal African trypanosomiasis disease. We assumed the same rate of host and vector migration in both patches. We set the control in patch 1 and 2 to be $u_1 = u_2 = 0$. Overall, we noted that the

number of new infections generated for livestock and wild animals in both patches are the same, that is 1.4014×10^3. From these results, one can note that there is no significant difference on spread of animal African Trypanosomiasis disease when the rate of migrations are the same in both patches.

3.1. Concluding remarks. In this work, a two-patch model that inter-plays between two hosts (Livestock and wild animals) and tsetse flies migration in seasonal variation has been proposed and systematically analyzed to assess the effect of host and vector movements in the dynamics of Animal trypanosomiasis transmission. The effect of treating livestock through spraying insecticides is incorporated in the model and its impact in reducing the spread of disease in the population has been investigated. In model analysis, the basic reproduction number R_0 that govern the spread of disease is computed in the periodic environment. Overall, we observed that it is possible to eradicate the animal African trypanosomiasis disease whenever the basic reproduction number R_0 is less than unity. We performed the numerical simulation of the model considering two scenarios: that is symmetrical and asymmetrical movement of both hosts and vectors. We observed that the solution profile of the model system for infected species is associated with the periodic oscillations which is caused by seasonal variation and migration of host and vectors. We have also noted that whenever the migration of hosts and vectors is asymmetrical, the number of infected species in both patches are not the same. In addition, we noted that treating the livestock with insecticides minimize the spread of disease in the population.

DATA AVAILABILITY

All data used in this paper included.

AUTHORS' CONTRIBUTIONS

All authors have equal contributions and they read and approved the final version of the paper.

CONFLICT OF INTERESTS

The author(s) declare that there is no conflict of interests.

REFERENCES

[1] A. Wesolowski, C.O. Buckee, K. Engø-Monsen, C.J.E. Metcalf, Connecting mobility to infectious diseases: The promise and limits of mobile phone data, J. Infect. Dis. 214 (2016), S414–S420. https://doi.org/10.1093/infdis/jiw273.

[2] S. Changruenngam, D.J. Bicout, C. Modchang, How the individual human mobility spatio-temporally shapes the disease transmission dynamics, Sci. Rep. 10 (2020), 11325. https://doi.org/10.1038/s41598-020-68230-9.

[3] M.L. Ndeffo-Mbah, A. Pandey, K.E. Atkins, et al. The impact of vector migration on the effectiveness of strategies to control gambiense human African trypanosomiasis, PLoS Negl. Trop. Dis. 13 (2019), e0007903. https://doi.org/10.1371/journal.pntd.0007903.

[4] J.W. Hargrove, A theoretical study of the invasion of cleared areas by tsetse flies (Diptera: Glossinidae), Bull. Entomol. Res. 90 (2000), 201–209. https://doi.org/10.1017/s0007485300000328.

[5] S. Moore, S. Shrestha, K.W. Tomlinson, H. Vuong, Predicting the effect of climate change on African trypanosomiasis: integrating epidemiology with parasite and vector biology, J. R. Soc. Interface. 9 (2011), 817–830. https://doi.org/10.1098/rsif.2011.0654.

[6] S.L. Peck, J. Bouyer, Mathematical modeling, spatial complexity, and critical decisions in tsetse control, J. Econ. Entom. 105 (2012), 1477–1486. https://doi.org/10.1603/ec12067.

[7] J.W. Hargrove, R. Ouifki, D. Kajunguri, et al. Modeling the control of trypanosomiasis using trypanocides or insecticide-treated livestock, PLoS Negl. Trop. Dis. 6 (2012), e1615. https://doi.org/10.1371/journal.pntd.0001615.

[8] S.F. Ackley, J.W. Hargrove, A dynamic model for estimating adult female mortality from ovarian dissection data for the tsetse fly Glossina pallidipes Austen sampled in Zimbabwe, PLoS Negl. Trop. Dis. 11 (2017), e0005813. https://doi.org/10.1371/journal.pntd.0005813.

[9] J.S. Lord, J.W. Hargrove, S.J. Torr, G.A. Vale, Climate change and African trypanosomiasis vector populations in Zimbabwe's Zambezi Valley: A mathematical modelling study, PLoS Med. 15 (2018), e1002675. https://doi.org/10.1371/journal.pmed.1002675.

[10] S. Alderton, E.T. Macleod, N.E. Anderson, et al. An agent-based model of tsetse fly response to seasonal climatic drivers: Assessing the impact on sleeping sickness transmission rates, PLoS Negl. Trop. Dis. 12 (2018), e0006188. https://doi.org/10.1371/journal.pntd.0006188.

[11] D.J. Rogers, A general model for the African trypanosomiases, Parasitology. 97 (1988), 193–212. https://doi.org/10.1017/s0031182000066853.

[12] C.M. Stone, N. Chitnis, Implications of heterogeneous biting exposure and animal hosts on trypanosomiasis brucei gambiense transmission and control, PLoS Comput. Biol. 11 (2015), e1004514. https://doi.org/10.1371/journal.pcbi.1004514.

[13] K.S. Rock, M.L. Ndeffo-Mbah, S. Castaño, et al. Assessing strategies against gambiense sleeping sickness through mathematical modeling, Clinic. Infect. Dis. 66 (2018), S286–S292. https://doi.org/10.1093/cid/ciy018.

[14] A.M. Ndondo, J.M.W. Munganga, J.N. Mwambakana, et al. Analysis of a model of gambiense sleeping sickness in humans and cattle, J. Biol. Dyn. 10 (2016), 347–365. https://doi.org/10.1080/17513758.2016.1190873.

[15] J.A. Gilbert, J. Medlock, J.P. Townsend, et al. Determinants of human African trypanosomiasis elimination via paratransgenesis, PLoS Negl. Trop. Dis. 10 (2016), e0004465. https://doi.org/10.1371/journal.pntd.0004465.

[16] K.S. Rock, S.J. Torr, C. Lumbala, M.J. Keeling, Predicting the impact of intervention strategies for sleeping sickness in two high-endemicity health zones of the Democratic Republic of Congo, PLoS Negl. Trop. Dis. 11 (2017), e0005162. https://doi.org/10.1371/journal.pntd.0005162.

[17] K.S. Rock, S.J. Torr, C. Lumbala, M.J. Keeling, Quantitative evaluation of the strategy to eliminate human African trypanosomiasis in the Democratic Republic of Congo, Parasites Vectors. 8 (2015), 532. https://doi.org/10.1186/s13071-015-1131-8.

[18] K.S. Rock, C.M. Stone, I.M. Hastings, et al. Mathematical Models of Human African Trypanosomiasis Epidemiology, in: Advances in Parasitology, Elsevier, 2015: pp. 53–133. https://doi.org/10.1016/bs.apar.2014.12.003.

[19] T. Madsen, D.i. Wallace, N. Zupan, Seasonal fluctuation in tsetse fly populations and human African trypanosomiasis: A mathematical model, Biomat. 2012 (2013), 56–69. https://doi.org/10.1142/9789814520829_0004.

[20] M. Helikumi, M. Kgosimore, D. Kuznetsov, S. Mushayabasa, Backward bifurcation and optimal control analysis of a trypanosoma brucei rhodesiense model, Mathematics. 7 (2019), 971. https://doi.org/10.3390/math7100971.

[21] N. Bacaër, S. Guernaoui, The epidemic threshold of vector-borne diseases with seasonality, J. Math. Biol. 53 (2006), 421–436. https://doi.org/10.1007/s00285-006-0015-0.

[22] W. Wang, X.-Q. Zhao, Threshold dynamics for compartmental epidemic models in periodic environments, J. Dyn. Differ. Equ. 20 (2008), 699–717. https://doi.org/10.1007/s10884-008-9111-8.

[23] M. Helikumi, M. Kgosimore, D. Kuznetsov, S. Mushayabasa, Dynamical and optimal control analysis of a seasonal Trypanosoma brucei rhodesiense model, Math. Biosci. Eng. 17 (2020), 2530–2556. https://doi.org/10.3934/mbe.2020139.

[24] R. Lowe, The impact of global environmental change on vector-borne disease risk: a modelling study, Lancet Planet. Health. 2 (2018), S1. https://doi.org/10.1016/s2542-5196(18)30086-x.

[25] H.J. Nnko, A. Ngonyoka, L. Salekwa, et al. Seasonal variation of tsetse fly species abundance and prevalence of trypanosomes in the Maasai Steppe, Tanzania, J. Vector Ecol. 42 (2017), 24–33. https://doi.org/10.1111/jvec.12236.

[26] P. Simarro, J. Franco, A. Diarra, J. Jannin, Epidemiology of human African trypanosomiasis, Clinic. Epidemiol. 6 (2014), 257-275. https://doi.org/10.2147/clep.s39728.

[27] World Health Organization, Control and surveillance of human African trypanosomiasis: report of a WHO expert committee, World Health Organization, Geneva, 2013. https://apps.who.int/iris/handle/10665/95732.

[28] World Health Organization, Human African trypanosomiasis (sleeping sickness): epidemiological update. Wkly Epidemiol. Rec. 8 (2006), 71–80. https://www.who.int/publications/i/item/who-wer-8108.

[29] S.G.A. Leak, Tsetse vector population dyanamics: ILRAD's Requirements. In: J.W. Hansen, B.D. Perry, (eds.) Modelling vector-borne and other parasitic diseases, International Livestock research institute (ILRI), (1994), 36 pp. https://books.google.co.zw/books?isbn=9290552972.

[30] L. Berrang-Ford, C. Wamboga, A.S.L. Kakembo, Trypanososma brucei rhodesiense Sleeping Sickness, Uganda, Emerg. Infect. Dis. 18 (2012), 1686–1687. https://doi.org/10.3201/eid1810.111213.

[31] N. Kelvin, E. Anna B, H. Peter J, G. Paul S, Influence of Seasonal Cattle Movement on Prevalence of Trypanosome Infections in Cattle in the Maasai Steppe, Tanzania, J Infect Dis Epidemiol. 5 (2019), 079. https://doi.org/10.23937/2474-3658/1510079.

[32] E.G. Kimaro, J.-A.L.M.L. Toribio, et al. Occurrence of trypanosome infections in cattle in relation to season, livestock movement and management practices of Maasai pastoralists in Northern Tanzania, Vet. Parasitol.: Region. Stud. Rep. 12 (2018), 91–98. https://doi.org/10.1016/j.vprsr.2018.02.007.

[33] S. Aksoy, P. Buscher, M. Lehane, et al. Human African trypanosomiasis control: Achievements and challenges, PLoS Negl Trop Dis. 11 (2017), e0005454. https://doi.org/10.1371/journal.pntd.0005454.

[34] P.P. Simarro, G. Cecchi, J.R. Franco, et al. Estimating and mapping the population at risk of sleeping sickness, PLoS Negl. Trop. Dis. 6 (2012), e1859. https://doi.org/10.1371/journal.pntd.0001859.

[35] P. Büscher, G. Cecchi, V. Jamonneau, G. Priotto, Human African trypanosomiasis, The Lancet. 390 (2017), 2397–2409. https://doi.org/10.1016/s0140-6736(17)31510-6.

[36] A.R. Cossins, K. Bowler, Temperature biology of animals, Springer Netherlands, 1987. https://doi.org/10.1007/978-94-009-3127-5.

[37] P. van den Driessche, J. Watmough, Reproduction numbers and sub-threshold endemic equilibria for compartmental models of disease transmission, Math. Biosci. 180 (2002), 29–48. https://doi.org/10.1016/s0025-5564(02)00108-6.

[38] G.O. Agaba, Y.N. Kyrychko, K.B. Blyuss, Dynamics of vaccination in a time-delayed epidemic model with awareness, Math. Biosci. 294 (2017), 92–99. https://doi.org/10.1016/j.mbs.2017.09.007.

[39] F.A. Basir, S. Ray, E. Venturino, Role of media coverage and delay in controlling infectious diseases: A mathematical model, Appl. Math. Comput. 337 (2018), 372–385. https://doi.org/10.1016/j.amc.2018.05.042.

[40] W. Randolph, K. Viswanath, Lessons learned from public health mass media campaigns: marketing health in a crowded media world, Annu. Rev. Public Health. 25 (2004), 419–437. https://doi.org/10.1146/annurev.publhealth.25.101802.123046.

[41] L.S. Pontryagin, V.T. Boltyanskii, R.V. Gamkrelidze, et al. The mathematical theory of optimal processes, Wiley, New Jersey, 1962.

[42] S. Lenhart, J.T. Workman, Optimal control applied to biological models, Chapman and Hall/CRC, London, 2007.

[43] D. Kirk, Optimal control theory: an introduction, Dover Publications, New York, 2012.

[44] X. Wang, Solving optimal control problems with MATLAB: Indirect methods, Technical Report, ISE. Dept., NCSU, Raleigh, NC 27695, (2009).

[45] D. Posny, J. Wang, Computing the basic reproductive numbers for epidemiological models in nonhomogeneous environments, Appl. Math. Comput. 242 (2014), 473–490. https://doi.org/10.1016/j.amc.2014.05.079.

[46] W. Wang, X.Q. Zhao, An epidemic model in a patchy environment, Math. Biosci. 190 (2004), 97–112. https://doi.org/10.1016/j.mbs.2002.11.001.

[47] X.Q. Zhao, Dynamical system in population biology, Springer-Verlag, New York, 2003.

[48] F. Zhang, X.Q. Zhao, A periodic epidemic model in a patchy environment, J. Math. Anal. Appl. 325 (2007), 496–516. https://doi.org/10.1016/j.jmaa.2006.01.085.

[49] X.Q. Zhao, Dynamical systems in population biology, Springer, New York, 2003.

[50] W.H. Fleming, R.W. Rishel, Deterministic and stochastic optimal control, Springer Verag, New York, 1975.

[51] D.W. Muia,S. Osman, M. Wainaina, Modelling and analysis of trypanosomiasis transmission mechanism, Glob. J. Pure Appl. Math. 14 (2018), 1311-1331.

[52] J. Pepin, H. Meda, The epidemiology and control of human African trypanosomiasis, in: Advances in Parasitology, Elsevier, 2001: pp. 71–132. https://doi.org/10.1016/S0065-308X(01)49038-5.

[53] Y.A. Liana, N. Shaban, G. Mlay, A. Phibert, African trypanosomiasis dynamics: Modelling the effects of treatment, education, and vector trapping, Int. J. Math. Math. Sci. 2020 (2020), 3690472. https://doi.org/10.1155/2020/3690472.

[54] R.C. Mattioli, U. Feldmann, G. Hendrickx, Tsetse and trypanosomiasis intervention policies supporting sustainable animal-agricultural development, J. Food Agric. Environ. 2 (2004), 310-314.

[55] P. Van den Bossche, S. de L. Rocque, G. Hendrickx, J. Bouyer, A changing environment and the epidemiology of tsetse-transmitted livestock trypanosomiasis, Trends Parasitol. 26 (2010), 236–243. https://doi.org/10.1016/j.pt.2010.02.010.

[56] E. Prowse, Trypanosomosis, the disease and its control : an analysis of a new tsetse-repellent technology. SLU, Dept. of Biomedical Sciences and Veterinary Public Health, Uppsala, 2005. http://urn.kb.se/resolve?urn=urn:nbn:se:slu:epsilon-s-7437.

[57] J.C. Devèze, In conclusion, a question: can tropical africa be a future agricultural giant? in: Challenges for African Agriculture, The International Bank for Reconstruction and Development/The World Bank, 2011.

[58] A.P.M. Shaw, G. Cecchi, G.R.W. Wint, et al. Mapping the economic benefits to livestock keepers from intervening against bovine trypanosomosis in Eastern Africa, Prevent. Vet. Med. 113 (2014), 197–210. https://doi.org/10.1016/j.prevetmed.2013.10.024.

[59]]M. Alsan, The effect of the tsetse fly on African development, Amer. Econ. Rev. 105 (2015), 382–410. https://doi.org/10.1257/aer.20130604.

[60] J. Otieno, J.Y.T. Mugisha, B.K. Nannyonga, et al. Parameter driven dynamics of trypanosomiasis in a cattle population, Appl. Math. Sci. 8 (2014), 2665-2685.

[61] D. Kajunguri, J.W. Hargrove, R. Ouifki, et al. Modelling the use of insecticide-treated cattle to control tsetse and trypanosoma brucei rhodesiense in a multi-host population, Bull. Math. Biol. 76 (2014), 673–696. https://doi.org/10.1007/s11538-014-9938-6.

[62] J. Meisner, R.V. Barnabas, P.M. Rabinowitz, A mathematical model for evaluating the role of trypanocide treatment of cattle in the epidemiology and control of Trypanosoma brucei rhodesiense and T. b. gambiense sleeping sickness in Uganda, Parasite Epidemiol. Control. 5 (2019), e00106. https://doi.org/10.1016/j.parepi.2019.e00106.

[63] J.S. Lord, R.S. Lea, F.K. Allan, et al. Assessing the effect of insecticide-treated cattle on tsetse abundance and trypanosome transmission at the wildlife-livestock interface in Serengeti, Tanzania, PLoS Negl. Trop. Dis. 14 (2020), e0008288. https://doi.org/10.1371/journal.pntd.0008288.